Structural Independence of Ligand-Binding Modules Five and Six of the LDL Receptor†

Christopher L. North‡ and Stephen C. Blacklow*,‡

Department of Pathology, Brigham and Women's Hospital and Harvard Medical School, 75 Francis Street, Boston, Massachusetts 02115

Received September 8, 1998; Revised Manuscript Received November 30, 1998

ABSTRACT: The low-density lipoprotein receptor (LDLR) is the primary mechanism for the uptake of plasma cholesterol into cells and serves as a prototype for a growing family of cell surface receptors. These receptors all utilize tandemly repeated LDL-A modules to bind their ligands. Each LDL-A module is about 40 residues long, has six conserved cysteine residues, and contains a conserved acidic region near the C-terminus which serves as a calcium-binding site. The structure of the interface presented for ligand binding by these modules, and the basis for their specificity and affinity in ligand binding, is not yet known. We have purified recombinant molecules corresponding to LDL-A modules five (LR5), six (LR6*), and the module five−six pair (LR5−6*) of the LDL receptor. Calcium is required to establish native disulfide bonds and to maintain the structural integrity of LR5, LR6*, and the LR5−6* module pair. Folding studies of the I189D and D206Y mutations within LR5 indicate that each change leads to misfolding of the module, explaining the previous observation that each of these changes mimics the functional effect of deletion of the entire module [Russell, D. W., Brown, M. S., and Goldstein, J. L. (1989) *J. Biol. Chem. 264*, 21682−21688]. By fluorescence, the affinity of LR5 for calcium, which is crucial for folding and function of these modules, remains ~40 nM whether LR6* is attached. Comparison of proton and multidimensional heteronuclear NMR spectra of individual modules to those of the module pair indicates that most of the significant spectroscopic changes lie within the linker region between modules and that little structural interaction occurs between the cores of modules five and six in the 5−6 pair. These findings strongly support a model in which each module is essentially structurally independent of the other.

The low-density lipoprotein receptor (LDLR)[1] is the primary mechanism for the uptake of cholesterol-carrying lipoproteins into cells. After the receptor−ligand complex is internalized through clathrin-coated pits, bound lipoprotein is released in the low pH environment of the endosome. The receptor is then returned to the cell surface by a process called receptor recycling (*1*). Mutations in the gene encoding the LDLR give rise to the genetic disease familial hypercholesterolemia (FH), which results in elevated plasma levels of LDL and cholesterol (*2*). Heterozygous FH, which affects approximately 1 in 500 persons, confers substantially increased risk for premature cardiovascular disease, and homozygous FH leads to death from coronary atherosclerosis at an early age (*2*).

The amino-terminal ligand-binding domain of the LDLR consists of seven tandemly repeated LDL-A modules (*3*). Each LDL-A module is about 40 residues long, has six conserved cysteine residues, and contains a conserved acidic region near the C-terminus which serves as a calcium-binding site (Figure 1). These LDL-A modules occur in a wide range of proteins including numerous cell-surface receptors (e.g., refs *4*−*8*) and components of the complement cascade (e.g., refs *9* and *10*).

Mutational studies of the seven LDL-A modules of the LDL receptor indicate that modules 3−7 all contribute significantly to binding of LDL particles (*11*), for which the predominant protein component is a single molecule of apolipoprotein B100. In contrast, only deletion of module five interferes with the ability of the receptor to bind β-VLDL particles, which contain multiple copies of apolipoprotein E (*11*). Remarkably, mutation of either of two conserved residues within any LDL-A module mimics the effect of deletion of that entire module (*11*).

Structures have been determined for LDL-A modules 1 and 2 of the LDLR by NMR (*12*, *13*), and an X-ray structure of module 5 (LR5) has been solved to a resolution of 1.7 Å (*14*). Each of these modules shares an unusual architecture, with little recognizable secondary structure. In the crystal

†This work was supported by the Program in Molecular and Genetic Medicine at Stanford University and by NIH Grant HL61001-01 (to S.C.B.). This work was conducted while Stephen C. Blacklow was a Pfizer Scholar.

* To whom correspondence should be addressed. Tel: (617) 732-5799. Fax: (617) 264-5296. E-mail: sblacklow@rics.bwh.harvard.edu.

‡ Department of Pathology.

[1] Abbreviations: amu, atomic mass unit; EDTA, ethylenediaminetetraacetic acid; EGTA, ethylene glycol-bis[β-aminoethyl ether]-*N*,*N*,*N*′,*N*′-tetraacetic acid; EGF, epidermal growth factor; FBML, Francis Bitter Magnet Laboratory; FH familial hypercholesterolemia; GSH, reduced glutathione; GSSG, oxidized glutathione; HPLC, high-pressure liquid chromatography; HSQC, heteronuclear single quantum coherence; Hz, hertz; LDL, low-density lipoprotein; LDLR, low-density lipoprotein receptor; LR1, LR2, LR5, LR6, first, second, fifth, and sixth LDL-A modules of the LDL receptor, respectively; LR6*, LR6 with the M243L point mutation; LR5−6, the LR5−LR6 module pair; LR5−6*, LR5−6 with the M243L point mutation; LRP, LDL receptor-related protein; ppm, parts per million; NTA, nitrilotriacetic acid; SH, Src homology; VLDL, very low-density lipoprotein.

10.1021/bi9821622 CCC: $18.00
Published on Web 03/11/1999

residue number	module	amino acid sequence
2-43	LR1	VGDR-C-ERNEFQCQD--GKCISYKWVCDGSAECQDGSDESQETCL
44-84	LR2	-SVT-C-KSGDFSCGGRVNRCIPQFWRCDGQVDCDNGSDEQG--CP
85-123	LR3	-PKT-C-SQDEFRCHD--GKCISRQFVCDSDRDCLDGSDEAS--CP
124-171	LR4	-VLT-C-GPASFQCNS--STCIPQLWACDNDPDCEDGSDEWPQRCRGLYVFQG
172-211	LR5	DSSP-C-SAFEFHCLS--GECIHSSWRCDGGPDCKDKSDEEN--CA
212-251	LR6	-VAT-C-RPDEFQCSD--GNCIHGSRQCDREYDCKDMSDEVG--CVN
252-292	LR7	--VTLCEGPNKFKCHS--GECITLDKVCNMARDCRDWSDEPIKEC
	consensus	---t-C-----F-C----g-CI-----CD---DC-D-SDE----C

FIGURE 1: Amino acid sequence of the ligand-binding domain of the LDL receptor. Numbering refers to residue position in the mature intact receptor. Sequences of the LR5 (residues 172−211) and LR6* (residues 212−251) constructs examined in this study are shaded in gray. The LR5−6* construct spans the entire gray region (172−251). The I189 and D206 residues of LR5 are indicated in bold; M243, which has been mutated to leucine in the LR6* and LR5−6* constructs, is on a white background. On the bottom row, consensus residues (boxed above) are indicated in upper case when conserved in at least 6 of the 7 modules, and in lower case when conserved in 5 of the 7 modules. Adapted from ref 11.

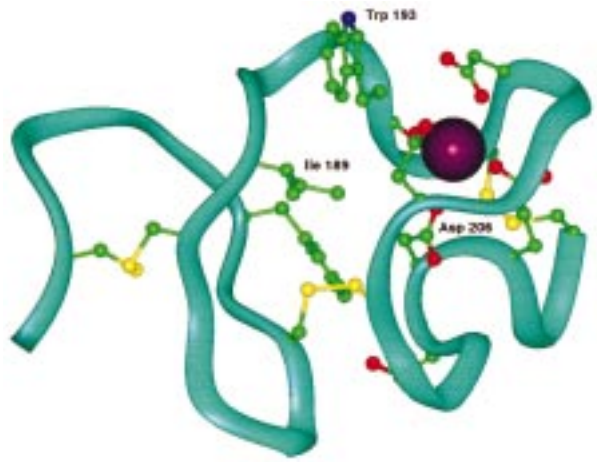

FIGURE 2: Ribbon diagram of the LR5 structure (*14*). Side chains of the cysteines, calcium-coordinating residues, conserved isoleucine, and conserved phenylalanine are included as reference points. The calcium ion is represented as a purple sphere. The figure was generated using Insight II (MSI Inc.) and adapted from ref 14.

structure of LR5 (Figure 2), six cysteine residues form three disulfide bonds (C1−C3, C2−C5, and C4−C6), constituting a scaffold which stabilizes the structure in conjunction with the calcium-binding site (*14*). Mutations of the calcium-coordinating residues result in FH, consistent with the known calcium requirement for receptor function (*15*) and folding (*16*, *17*).

The LDLR serves as a prototype for an expanding family of cell-surface receptors (see ref *18* for a recent review). These proteins which include the LRP (*7*), gp330 (*5*), and the VLDL receptors (*4*, *6*), share a modular domain organization similar to that of the LDLR. In members of the LDLR gene family, the LDL-A modules always occur in stretches of multiple repeats.

Previous studies are consistent with two models for the role of module interaction of these multiple repeats in ligand binding. In one model, specific residues in structurally independent modules are more important for receptor function than module organization. In the other, intermodular organization and spacing play the most important role in ligand recognition. A recent report, which suggests LDL-A modules 1 and 2 do not interact strongly with each other (*19*), supports the first model. However, these modules are the least important for lipoprotein binding in functional studies (*11*).

The purpose of these studies has been to investigate the relationship between functionally important adjacent LDL-A modules of the LDLR. Is each LDL-A module an independent structural element, or is there a well-defined intermodule organization which is required to present a structured binding interface? We have addressed this question using modules five (LR5) and six (LR6*, which harbors the M243L substitution to facilitate protein expression) and the 5−6* pair (LR5−6*) of the LDLR as a model.

Here, we show that calcium is required to establish and maintain the structural integrity of LR5 (see also ref *17*), LR6*, and the LR5−6* module pair. The Ca^{2+} affinity of module 5, measured by fluorescence spectroscopy, is not altered in the LR5−6* module pair, suggesting that modules five and six within the pair are structurally independent. Furthermore, comparison of proton and multidimensional heteronuclear NMR spectra of individual modules to those of the module pair indicates that the significant spectroscopic changes lie within the linker region between modules. Taken together, these findings strongly support a model in which each module is essentially structurally independent of the other.

EXPERIMENTAL PROCEDURES

Protein Expression and Purification. Plasmid pLDLR2 (*3*), which contains the gene encoding the human LDLR, was obtained from the American Type Culture Collection (Rockville, MD). Cassettes encoding residues 172−211 (LR5), 212−251 with a M243L mutation (LR6*), and 172−251 with a M243L mutation (LR5−6*) of the LDLR, each flanked by *Hin*dIII and *Bam*H1 restriction sites, were constructed by the polymerase chain reaction using appropriate oligonucleotides. Each cassette was subcloned into the vector pMMHb (a kind gift of M. Milhollen, Whitehead Institute). In the resulting plasmids, denoted pMM-LR5, pMM-LR6*, and pMM-LR5−6*, the LDL-A modules are expressed as a fusion with a modified form of the trpLE sequence in which the methionine and cysteine residues have been replaced by leucine and alanine, respectively (*17*), and an amino-terminal $(His)_9$ tag has been added, creating a $(His)_9$−TrpLE−Met−LRX chimeric protein (where X is 5, 6*, or 5−6*). Standard recombinant DNA techniques were used (*20*). The identity of each construct was confirmed by DNA sequencing. The mutations I189D and D206Y in LR5 were generated by Kunkel mutagenesis (*21*) and confirmed by DNA sequencing.

Unlabeled protein was expressed in LB (DIFCO); uniformly ^{15}N-labeled protein was expressed in M9 minimal media using $^{15}NH_4Cl$ as the sole nitrogen source (*22*). Each chimeric protein, expressed in *Escherichia coli* strain BL21-(DE3) pLys(S) (*23*) is found in inclusion bodies. The inclusion bodies were isolated and purified from the cell pellet as described (*17, 24*) and then dissolved in 10 mM tris buffer, pH 8.0, containing 6.0 M guanidine HCl and 10 mM oxidized 2-mercaptoethanol. After oxidation overnight at room temperature, the sample was batch loaded onto a column of Ni^{2+}-NTA agarose (Qiagen; Chatsworth, CA). Each fusion protein was eluted with a solution of 10 mM tris buffer, pH 6.3, containing 6.0 M guanidine HCl and 300 mM imidazole, dialyzed exhaustively against 5% acetic acid, and lyophilized to dryness.

The lyophilized fusion protein was cleaved with cyanogen bromide, dialyzed exhaustively against 5% aqueous acetic acid after cleavage, and lyophilized to dryness. The dry protein was dissolved in 10 mM Tris buffer, pH 8, containing 8 M urea. After the $(His)_9$-TrpLE was removed by passage over a column of Ni^{2+}-NTA agarose, the recovered protein was dialyzed against a redox buffer of 10 mM Tris, pH 8.5, containing 2 mM reduced glutathione, 1 mM oxidized glutathione, and 10 mM $CaCl_2$, at 4 °C. Following three buffer changes over a 72 h period, the refolded protein was purified by reversed-phase HPLC using a C18 column. The identities of LR5, LR6*, and LR5−6* were confirmed by MALDI-TOF mass spectrometry (Voyager Elite, PerSeptive Biosystems). All observed masses were within 3 amu of the expected value. Purified peptides were stored in lyophilized form at 4 °C.

Disulfide Exchange Experiments. The calcium dependence of folding was investigated for each protein under conditions permitting disulfide exchange. Oxidized LR5, LR6*, or LR5−6* (3−4.5 μM) was allowed to rearrange at 4 °C in a redox buffer of 10 mM tris, pH 8.5, containing reduced glutathione (GSH; 2.5 mM), oxidized glutathione (GSSG; 0.5 mM), and either $CaCl_2$ (2 mM) or EDTA (2 mM).

With a similar protocol, the I189D and D206Y mutants of LR5, previously utilized in functional studies of ligand-binding by the LDLR (*11*), were evaluated for their ability to form native disulfide bonds. Reduced wild-type and mutant LR5 peptides (10 μM) were equilibrated at room temperature in a redox buffer of 50 mM tris, pH 8.5, containing GSH (2 mM) and GSSG (1 mM) and either $CaCl_2$ (1 mM) or EDTA (1 mM).

Aliquots were removed from each sample at 24 and 48 h; disulfide exchange was stopped by addition of acetic acid to a final concentration of 5% (v/v). Samples were analyzed by reversed-phase HPLC on a Vydac C-18 column using a linear gradient of 0.1%/minute of solvent B. Solvent reservoirs contained water with 0.1% trifluoroacetic acid (A) and 90% acetonitrile with 0.1% trifluoroacetic acid (B).

Comparison of 24 and 48 h time points suggests that an equilibrium distribution of disulfide-bonded isomers is reached within 24 h. In addition, no difference in the distribution of isomers is observed for wild-type LR5 regardless of whether the rearrangement is initiated with reduced or oxidized protein.

The distribution of products from folding of wild-type LR5, starting with reduced peptide and using EDTA in place of calcium in the folding buffer, was purified by HPLC in a single fraction for one-dimensional NMR. For NMR spectroscopy of the D206Y and I189D mutants of LR5, large-scale preparations of these proteins were first purified by HPLC in reduced form. After lyophilization, the mutants (∼50 μM) were allowed to refold in folding buffer (5 mL) for 48 h at 4 °C. The resulting distribution of oxidized products was purified by HPLC. The distribution of products from the I189D folding reaction eluted as a broad unresolved peak from the preparative column and was collected in a single fraction for NMR. The products of the D206Y folding reaction were collected in three fractions, each providing enough material for one-dimensional NMR. The first fraction was a sharply defined peak comprising ∼25% of the total material, corresponding to the 45−51 min period of the analytical HPLC time trace presented in Figure 3E. Note that the large-scale preparation of D206Y, folded at 4 °C, yielded more of this sharp, early eluting peak. The second and third fractions contain protein corresponding to the 51−54 and 55−61 min period of Figure 3E.

Fluorescence Measurements of Calcium Affinity. The Ca^{2+} affinity constants of LR5, LR6*, and LR5−6* were determined by observing changes in the relative fluorescence emission intensity of tryptophan 193 (LR5 and LR5−6*) and tyrosine 239 (LR6*). Spectra were acquired on an Aminco model AB2 fluorescence spectrometer by excitation at 280 nm, monitoring relative emission at 350 nm (LR5 and LR5−6*) or at 303 nm (LR6*). Protein concentrations of 0.2 μM (LR5 and LR5−6*) and 2 μM (LR6*) were used. Aliquots of an atomic absorption standard calcium solution (incrementing total calcium concentration by 10 μM in each step) were added to a solution of native protein in 10 mM PIPES buffer, pH 7.0, containing 100 mM NaCl and 0.1 mM EGTA. The EGTA-buffered concentration of free Ca^{2+} in the solution (0−2.1 μM) was calculated using the program MaxChelator (v. 6.50; *25*).

One-Dimensional Proton NMR Spectroscopy. Proton NMR spectra of wild-type LR5, LR6*, and LR5−6* were obtained at 11.75 T using a Varian Unity spectrometer at 25 °C. Samples of LR5, LR6*, and LR5−6* were prepared at protein concentrations of ∼2 mM in 90% H_2O/10% D_2O, pH 5.2, in the absence of added buffer or salt. Sixty-four transients of 2048 points with a 7000 Hz sweep width were acquired for each sample using WATERGATE water suppression (*26*). Residual unsuppressed solvent signal was removed by convolution; 1 Hz of line broadening was applied to the data before zero filling to 4096 points. Spectra were referenced to water at 4.76 ppm.

Proton NMR spectra of LR5, folded in the absence of calcium and of the I189D and D206Y mutants, were obtained at 9.4 T using a Varian Unity Plus spectrometer at 25 °C. Samples were prepared at protein concentrations of ∼0.5 mM in 90% H_2O/10% D_2O, pH 5.2, in the absence of added buffer or salt. A total of 256 transients of 2048 points with a 5600 Hz sweep width were acquired for each sample using WATERGATE solvent supression (*26*). Residual unsuppressed solvent signal was removed by convolution; 1 Hz of line broadening was applied to the data before zero filling to 4096 points. A first spectrum was acquired in the absence of calcium, and then a second spectrum was acquired after 10 mM $CaCl_2$ was added to each sample.

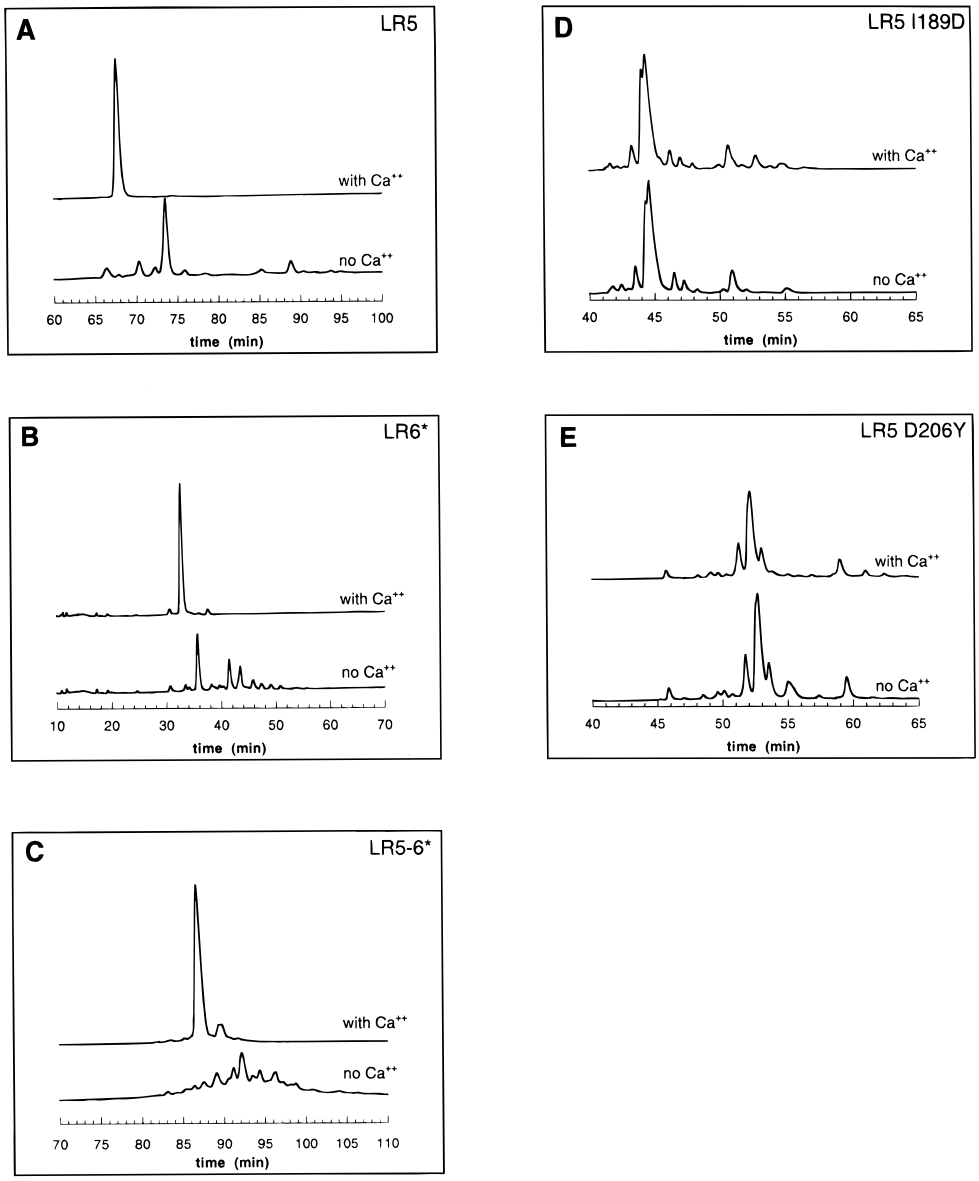

FIGURE 3: HPLC chromatograms of products formed after folding of LR5 (A), LR6* (B), LR5−6* (C), the I189D mutant of LR5 (D), and the D206Y mutant of LR5 (E). Folding of wild-type LR5, LR6*, and LR5−6* in the presence of calcium (A−C, top trace) yields predominantly the native disulfide isomer; whereas folding in the absence of calcium (A−C, bottom trace) produces a distribution of non-native disulfide-bonded species. Folding of the I189D (D) and D206Y (E) mutants of LR5 do not oxidize to a unique disulfide isomer, and the observed distribution of isomers is virtually identical when folding is performed in the presence (top) and absence (bottom) of calcium.

Heteronuclear ^{15}N-^{1}H NMR Spectroscopy. 2D HSQC spectra (*27*) were obtained at 11.75 T on uniformly ^{15}N-labeled protein in 10% D_2O at pH 5.2 and 25 °C in the absence of added buffer or salt. A total of 1024 × 256 complex points were acquired with sweep widths of 7000 Hz in D1 (^{1}H) and 3200 Hz in D2 (^{15}N). A 60° shifted-sine squared function was applied to the data in D1, and a 90° shifted sine-function was applied in D2.

Sequence-specific assignments were determined from 3D TOCSY−HSQC (τ_{mix} = 75 ms) and 3D NOESY-HSQC (τ_{mix} = 150 ms) spectra obtained at 11.75 T on Varian Unity (LR5 and LR6*) and home-built FBML (LR5−6*) spectrometers as 512 × 32 × 128 complex points with sweep widths of 7000 × 3200 × 7000 Hz in the D1, D2 (^{15}N), and D3 dimensions. A 60° shifted sine-squared function was applied to the data in D1, and a 90° shifted sine function was applied in D2 and D3. Linear prediction was used to extend data in the ^{15}N dimension to 64 points. WATERGATE suppression of the water resonance was used (*26*). All spectra were processed using Felix 97.0 software (MSI Inc.).

RESULTS

Calcium Requirement for Formation of Native Disulfide Bonds. The role of calcium in guiding formation of native disulfide bonds in LR5, LR6*, and LR5−6* was investigated under conditions permitting disulfide exchange. Purified LR5, LR6, and LR5−6* were allowed to equilibrate in the presence and absence of Ca^{2+} in a redox buffer. The resulting distribution of disulfide bonded isomers was resolved by reversed-phase HPLC.

In the presence of Ca^{2+}, a single predominant species representing the native disulfide isomer is observed (Figure 3, panels A−C top trace). In the absence of Ca^{2+}, HPLC

traces reveal a mixture of species reflecting the formation of a distribution of nonnative disulfide isomers for each peptide (Figure 3, panels A−C, bottom trace). LR5 containing the point mutations I189D and D206Y, which have been shown to produce effects similar to module deletion in functional studies (*11*), are insensitive to the presence of Ca^{2+} and fail to form a single disulfide isomer (Figure 3, panels D−E).

Measurements of Calcium Affinity by Fluorescence. The fluorescence emission signals of tryptophan 193 of LR5 and tyrosine 239 of LR6* increase in response to the structural changes caused by the binding of Ca^{2+} to these modules. Because LR6* contains no tryptophan residues, tryptophan 193 also provides a probe of Ca^{2+} binding to the LR5 module in the LR5−6* pair. With excitation at 280 nm, the relative emission intensity at 350 nm for tryptophan and 303 nm for tyrosine, was fit to the equation of saturating binding as a function of free Ca^{2+} (eq 1):

$$F_{Ca^{++}_{free}} - F_0 = \frac{(F_m - F_0) \times [Ca^{++}_{free}]}{K_d + [Ca^{++}_{free}]} \qquad (1)$$

The K_d for the binding of Ca^{2+} by LR5 is 36 ± 5 nM (Figure 4A), while the K_d for Ca^{2+} of LR5 within LR5−6*, 44 ± 7 nM (Figure 4B), is not significantly different from that of LR5 alone. The K_d of the LR6* module for Ca^{2+}, measured by tyrosine fluorescence, is 203 ± 24 nM (Figure 4C).

One-Dimensional Proton NMR of Wild-Type LR5, LR6, and LR5−6*.* In the absence of well-defined structure, chemical shifts tend toward the values observed in random coil peptides. Conversely, well-defined structure results in increased chemical shift dispersion because protons are positioned in unique local environments.

To address the role of calcium coordination in maintaining the structural integrity of individual modules and of the LR5−6* pair, 1D proton NMR spectra were acquired in the presence and absence of calcium. The 1D proton spectra of refolded LR5, LR6*, and the LR5−6* pair demonstrate dramatic increases in chemical shift dispersion in response to Ca^{2+} (Figure 5), particularly in the amide region. Furthermore, two methyl resonances of LR6*, with chemical shifts of ~1 ppm in the sample without Ca^{2+}, move upfield to 0.56 and 0.23 ppm in the presence of Ca^{2+}(compare Figure 5C with Figure 5D). These observations demonstrate that the LR5 and LR6* modules require Ca^{2+} not only to guide formation of correct disulfide bonds (Figure 3) but also to maintain a single well-defined structure in solution.

Comparison of the spectrum predicted by addition of the individual LR5 and LR6* spectra with the observed spectrum of LR5−6* shows only small differences (compare Figure 5F with Figure 5G). Furthermore, resolved resonances in the spectra of each individual module are generally found unchanged in the spectrum of the module pair, suggesting that each module is structurally independent of its neighbor.

One-Dimensional Proton NMR of Nonnative LR5 Isomers and of the I189D and D206Y Mutants of LR5. Wild-type LR5, folded in the absence of calcium, yields a distribution of nonnative disulfide-bonded isomers similar to that observed in denaturant (*17*; see also Figure 3A). Disulfide assignment of the predominant isomer formed by LR5 after

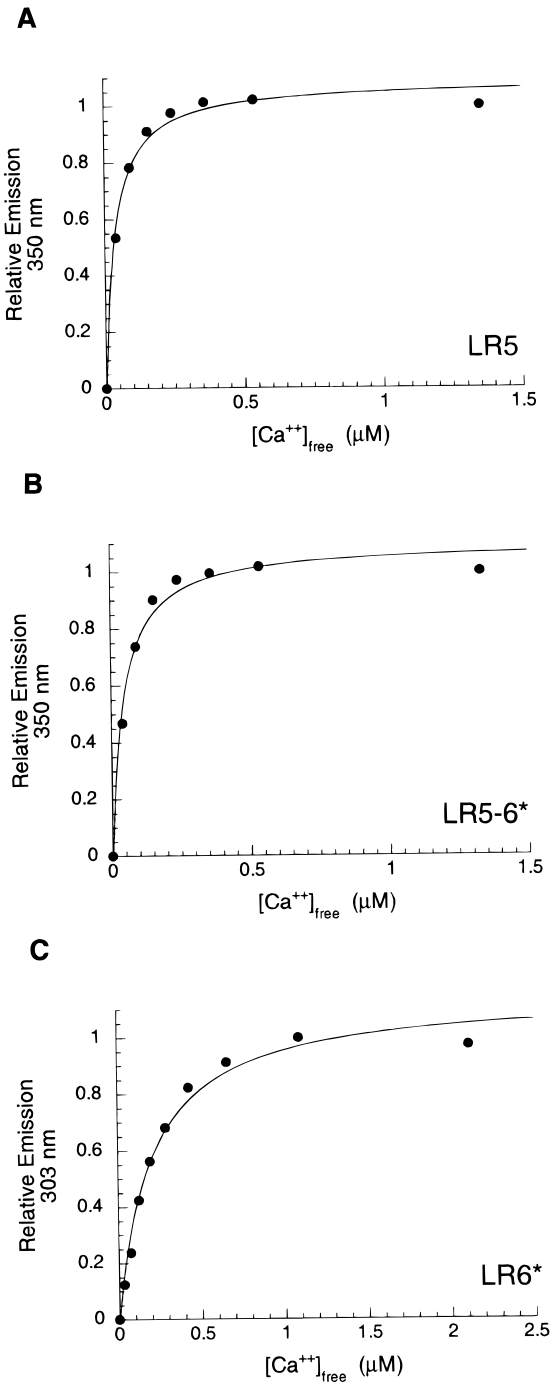

FIGURE 4: Calcium binding curves of LR5 (A), of the LR5 site within LR5−6* (B), and of LR6* (C), measured by fluorescence. Emission was monitored at 350 nm (A, B) or 303 nm (C) after excitation at 280 nm. To determine calcium-binding constants, curve fits were performed as described in the Experimental Procedures.

equilibration in denaturant indicates the presence of nonnative disulfide bonds (*17*). To confirm that nonnative disulfide isomers of wild-type LR5 are indeed misfolded, these forms of LR5, purifed as a broad unresolved peak by preparative HPLC, were investigated by one-dimensional NMR. In contrast to wild-type LR5 with native disulfide bonds, which shows a marked increase in chemical shift dispersion after the addition of calcium (Figure 5B), the nonnative forms of LR5 have little chemical shift dispersion in the amide region and do not exhibit changes in the NMR spectrum after the addition of calcium (Figure 6A). Furthermore, the presence

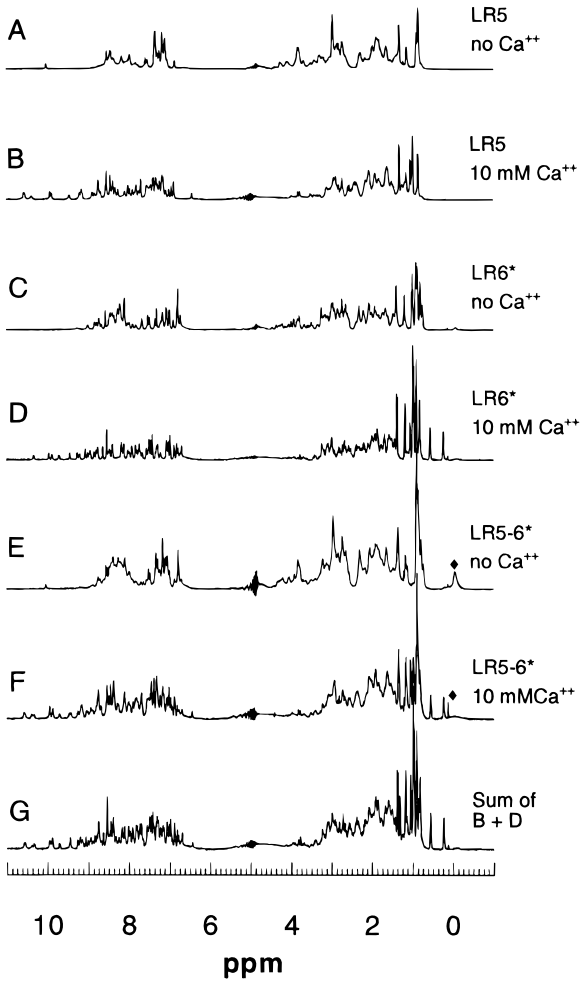

FIGURE 5: One-dimensional NMR spectra of LR5, LR6*, and LR5−6* performed in the presence and absence of calcium. LR5 without calcium (A); LR5 after addition of calcium (B); LR6* without calcium (C); LR6* after addition of calcium (D); LR5−6* without calcium (E); LR5−6* after addition of calcium (F); Spectrum calculated (G) from the sum of B (LR5 with calcium) and D (LR6* with calcium). In the spectra without calcium (A, C, and E), the chemical shift dispersion is poor; after the addition of calcium (spectra B, D, and F), a marked increase in chemical shift dispersion is observed. Impurities in spectra E and F are indicated by a diamond.

of more than one tryptophan indole resonance at ~10 ppm, even though there is only one tryptophan residue in the LR5 amino acid sequence, indicates that several different disulfide isomers are present within the misfolded sample.

Unlike wild-type LR5, the I189D and D206Y mutants fail to form a unique disulfide isomer even when folded in the presence of calcium (Figure 3, panels D and E). After HPLC purification, the products of the folding reactions of these mutants were also examined by NMR. The spectroscopic features of the I189D preparation resemble those of wild-type LR5-folded in the absence of calcium: (i) there is little chemical shift dispersion in the amide region, (ii) there are no changes in the NMR spectrum after the addition of calcium, and (iii) there are several distinguishable tryptophan indole resonances at ~10 ppm, even though there is only one tryptophan residue in the LR5 amino acid sequence (Figure 6B). These observations indicate that I189D misfolds to a distribution of nonnative disulfide isomers, none of which resemble the native fold of wild-type LR5.

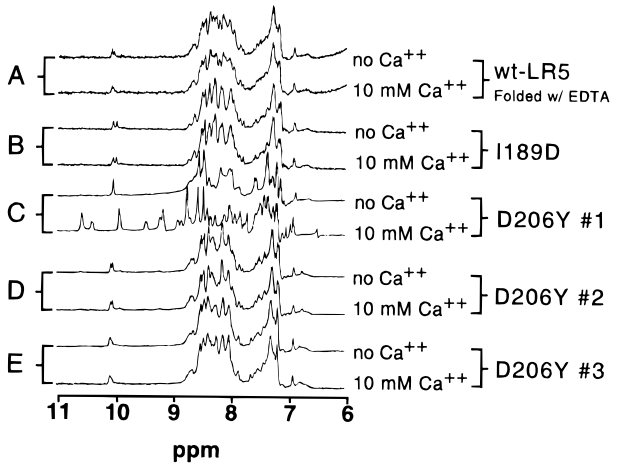

FIGURE 6: (A) One-dimensional NMR spectra of the products of folding when wild-type LR5 is allowed to equilibrate in disulfide exchange buffer in the absence of calcium. (Top) Spectrum without calcium; (bottom) spectrum after addition of calcium. In contrast to wild-type LR5 with native disulfide bonds, the nonnative disulfide isomers of LR5 have little chemical shift dispersion in the amide region and do not exhibit spectral changes after the addition of calcium (compare with Figure 5, panels A and B). Spectra of the products of folding when the I189D (B) and D206Y (C−E) mutants of wild-type LR5 are allowed to equilibrate in disulfide exchange buffer in the presence of calcium. The spectroscopic features of I189D (B) resemble those of wild-type LR5-folded in the absence of calcium (A). The folding reaction of D206Y could be resolved into three fractions by HPLC; each of these fractions was examined by NMR. Comparison of the NMR spectra of each fraction before (top) and after (bottom) the addition of calcium shows that only the first (C) of these fractions exhibits the characteristic changes in chemical shift dispersion observed for natively folded LR5; the spectroscopic features of the other two fractions (D, E) resemble those of wild-type LR5-folded in the absence of calcium (A).

The folding reaction of D206Y yielded a distribution of products that could be resolved into three fractions by preparative HPLC; each of these fractions was examined by NMR. Comparison of the NMR spectra of each fraction before and after the addition of calcium shows that only the first of these three fractions (representing ~25% of the total protein when folded at 4 °C, and less that 10% of the total protein when folded at 25 °C) exhibits the characteristic changes in chemical shift dispersion observed for natively folded LR5 (Figure 6, panels C−E).

Heteronuclear NMR Spectroscopy of LR5, LR6, and LR5−6**. The correlated ^{1}H-^{15}N chemical shifts of HSQC spectra provide a more sensitive probe of changes in protein structure. Thus, to investigate further the interactions between adjacent modules, we expressed and purified ^{15}N-labeled LR5, LR6*, and LR5−6*. With few exceptions, the resonances in the HSQC spectra of LR5 and LR6* overlay with those in the HSQC spectrum of LR5−6* (Figure 7).

Sequential assignments and differences in α proton chemical shifts were determined from 3D TOCSY-HSQC and 3D NOESY-HSQC experiments. The largest chemical shift differences of Hα proton resonances between individual modules and the module pair occur in the residues at the junction between the two modules (Figure 8).

DISCUSSION

The low-density lipoprotein receptor (LDLR) is the primary mechanism for the uptake of plasma cholesterol into

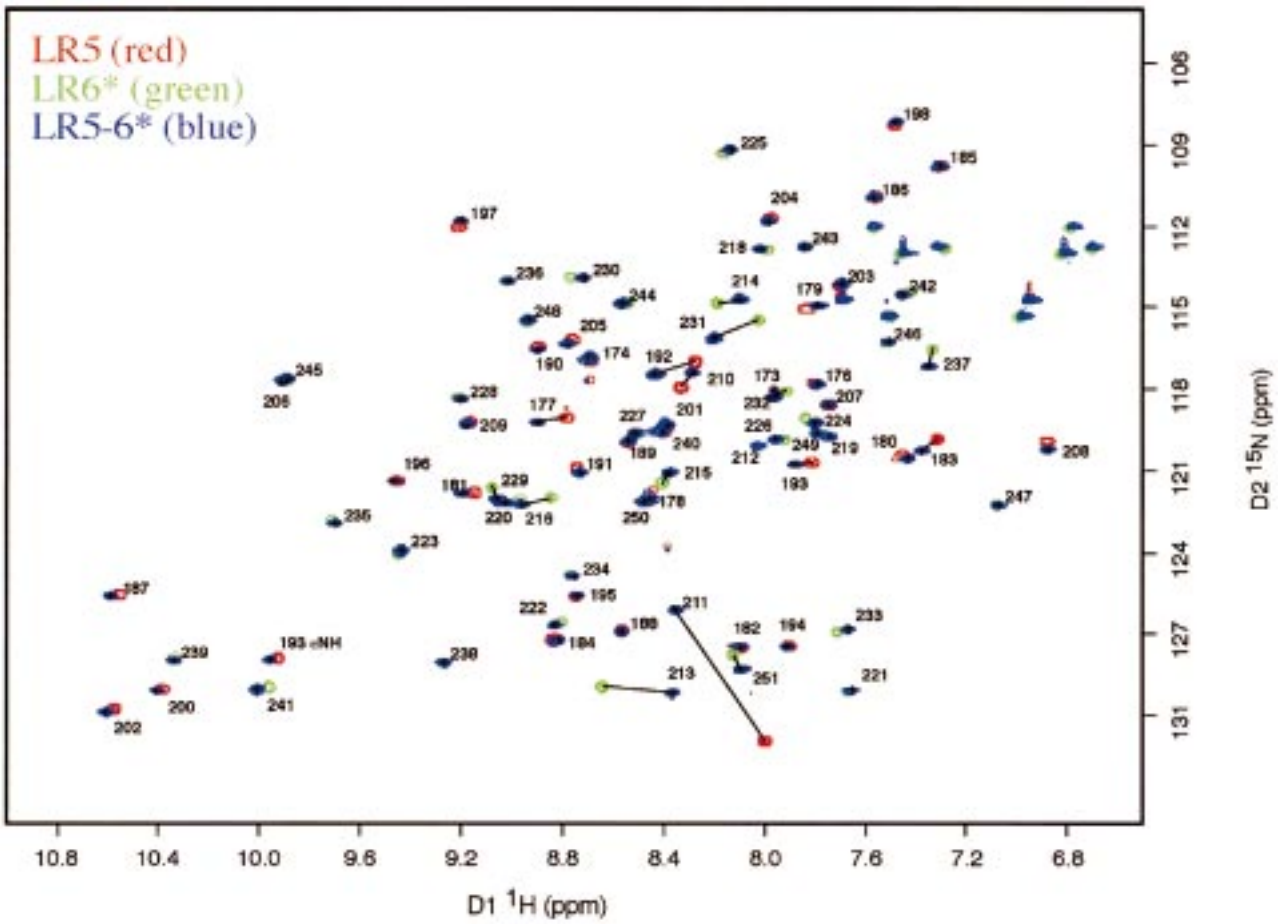

FIGURE 7: Assigned ^{15}N-^{1}H HSQC spectra of LR5 (red), LR6* (green), and LR5−6* (blue), overlaid on one another. Spectra were acquired in the presence of Ca^{2+} (10 mM) at pH 5.2 and 25 °C as described in the Experimental Procedures. Lines connect resonances that shift in the LR5−6* module pair relative to corresponding resonances in LR5 and LR6*.

cells and serves as a prototype for a growing family of cell surface receptors. These receptors all utilize tandemly repeated LDL-A modules to bind ligands. The structure of the interface presented for ligand binding by these modules, and the basis for their specificity and affinity in ligand binding, is not yet known.

Different combinations of LDL-A modules mediate binding of the LDLR to apolipoprotein B- and apolipoprotein E-containing lipoproteins (*11*). To begin development of a detailed model for how the LDLR might present its lipoprotein-binding domain on the cell surface, we have investigated the interface between LR5 and LR6, an adjacent pair of functionally important modules from the LDLR ligand-binding domain.

Properties of Individual Modules. A number of individual LDL-A modules, including LR1 (*12*), LR2 (*13*), and LR5 (*14, 17*) have been studied in isolation from the rest of the receptor. For each module, Ca^{2+} is required for in vitro formation of the native disulfide isomer, which always follows the pattern C1−C3, C2−C5, and C4−C6 (*17, 28, 29*). The X-ray crystal structure of LR5 contains a calcium ion coordinated by a cluster of conserved acidic residues that lie at the carboxy terminus of the module (*14*; Figure 2); the presence of the conserved calcium-binding site explains the calcium requirement for in vitro folding of LDL-A modules (*16, 17*; Figure 3) and reveals the basis for misfolding of mutants of LR1 (*30*) and LR5 (*17*) found in FH.

In functional studies of the LDLR by mutagenesis, point mutation of either of two residues within any repeat, a I → D mutation of the conserved isoleucine, and a D → Y mutation of the conserved aspartate of the DCxDxS**D**E sequence, mimicked the effect of deletion of the repeat (*11*). However, whether each point mutation affected the structure of the altered LDL-A module remained unknown.

Here, the I189D and D206Y mutations within LR5 were purified after expression as recombinant domains in *E. coli*. Each was permitted to fold under redox conditions that result in quantitative refolding of wild-type LR5. Neither I189D nor D206Y fold to a single disulfide isomer (Figure 3, panels D and E); the observed distribution of isomers is similar regardless of whether calcium is included in the folding buffer, suggesting that misfolding of each mutant is coupled to a defect in calcium coordination. NMR spectroscopy of the distribution of products from these folding reactions confirms this interpretation (Figure 6). As a result, any observed change in ligand affinity in these mutated proteins is likely a secondary consequence of misfolding, rather than the direct result of an alteration of an intimate contact with ligand.

Calcium Requirement for Structural Integrity. Ligand-binding by the LDLR requires calcium. Proton NMR studies, which indicate that Ca^{2+} is necessary to establish and

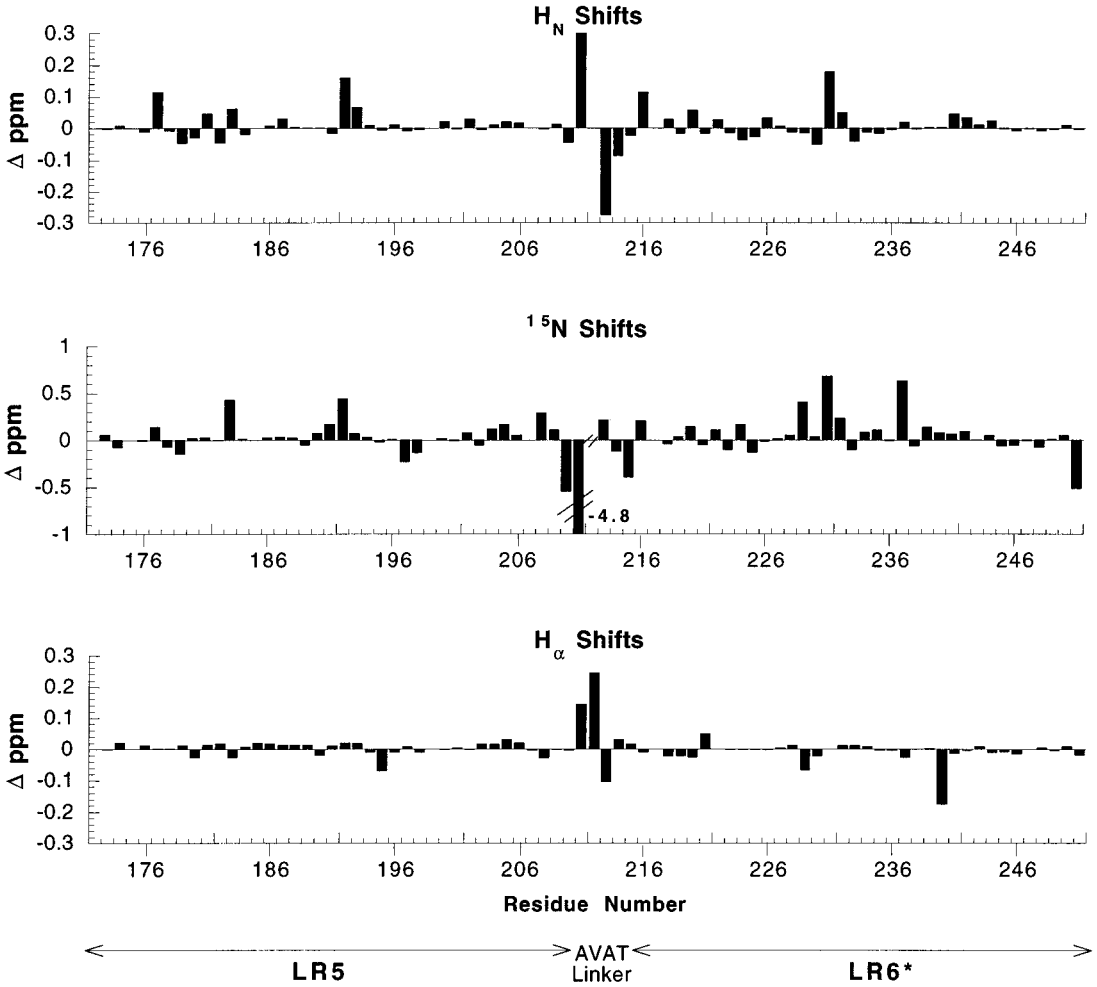

FIGURE 8: ^{15}N (A), H_N (B), and Hα (C) chemical shift differences between resonances of LR5−6* and corresponding resonances of LR5 and LR6*. Values for proline residues (175, 199, and 217), which lack H_N protons, are not reported. Because valine 212 lies at the N-terminus of LR6*, a chemical shift difference for its ^{15}N and H_N frequencies is also not reported.

maintain module structure, provide a rationale for why ligand binding by the LDLR depends on calcium. With native disulfide bonds already in place, LR1 (*16*), LR5 (*17*; compare Figure 5A with Figure 5B), LR6* (compare Figure 5C with Figure 5D), and LR5−6* (compare Figure 5E with Figure 5F) demonstrate dramatic spectroscopic changes after the addition of Ca^{2+}. Only after the addition of calcium are the spectra characteristic of folded proteins, with marked increases in chemical shift dispersion and sharpened resonance lines.

These findings are also consistent with the recent demonstration that a model for the ligand-binding domain expressed in insect cells acquires increased resistance to proteolysis and decreased susceptibility to reducing agents after the addition of calcium (*31*). Taken together, these observations suggest that the calcium requirement for structural integrity is a general characteristic of LDL-A modules, and that the calcium coordinating core is crucial in determining both structure and function of individual modules.

Structural Independence of Individual Modules in the LR5−6 Pair*. Structural studies of adjacent pairs of other types of small modules have revealed that the interfaces between repeat units can be flexible or rigid (see ref 32 for a recent review). The other type of calcium-coordinating modules that have been studied as a contiguous pair by NMR are epidermal growth factor (EGF) modules. In the module 32−33 pair from human fibrillin-1 (*33*, *34*), a conserved tyrosine residue in the linker between modules stabilizes the intermodule interface and establishes a precise orientation of one module with respect to the next (*34*). The calcium affinity of the module 33 site, which lies adjacent to the interface, is much stronger than that of the distant module 32 site (*33*). The authors attribute this difference in affinity to stabilization of the calcium coordination site in module 33 by the well-packed interface and to protection of the site from solvent by the adjacent module.

A large number of cell-surface molecules also contain LDL-A modules in tandemly repeated stretches. The length of the linker from one module to the next is frequently conserved and a threonine residue in the linker often precedes the first cysteine of the next module (Figure 1). These conserved sequence features suggest the possibility that general principles also govern the structural relationship between adjacent LDL-A repeats. To address this possibility, we have investigated the relationship between LR5 and LR6, an adjacent pair of ligand-binding modules from the LDLR. This pair of modules is critical for lipoprotein binding and exhibits the conserved linker motif.

Several lines of evidence support the hypothesis that the structure of each module of the LR5−LR6* pair is largely unaffected by the presence of its neighbor. First, the affinity

of LR5 for calcium remains essentially the same whether LR6* is also attached (compare Figure 4A with Figure 4B). This finding indicates that each module has an independent calcium-coordination site that is unperturbed by the neighboring module. In addition, the one-dimensional NMR spectrum of the LR5−LR6* module pair is very similar to that predicted by simple addition of the spectra of individual modules LR5 and LR6* (compare Figure 5F with Figure 5G).

The interface between the two modules was investigated in greater detail by NMR after sequential assignment of ^{15}N-labeled LR5, LR6*, and LR5−LR6*. With few exceptions, resonances from each single-module ^{1}H-^{15}N HSQC spectrum superimpose on those from the LR5−LR6* HSQC spectrum (Figure 7). Outside of the linker, only serine 192 of LR5 and serine 231 of LR6*, which are comparably positioned in each module (Figure 1), have substantially altered ^{15}N and $^{1}H_N$ (>0.1 ppm) chemical shifts in the LR5−6* module pair (Figure 8, panels A and B). However, when the Hα chemical shift of either of these residues in its individual module is compared with its value in the module pair, no significant difference is observed (Figure 8C). Significant perturbations (>0.1 ppm) of the LR5 and LR6 Hα chemical shifts only occur for the two residues at the junction between modules in the linker region (A211 and V212) and for C240 of module 6, indicating that there is little direct contact between LR5 and LR6* in the module pair. The authors of a recent study of LDLR modules 1 and 2 also see little change when the Hα chemical shifts of individual modules 1 and 2 are compared with those of the module pair (*19*), findings fully consistent with those reported here.

Even though few intermodule interactions are observed in either the LR5−LR6 or the LR1−LR2 module pair (*19*), neither of these studies addresses whether all of the modules of the LDLR are incorporated into an organized global topology. In the kinase Lck, the consecutive SH2 and SH3 domains make little contact with each other when studied in the absence of the remainder of the protein (*35*). However, in the structure of larger fragments of the related kinases c-Src (*36*) and Hck (*37*) that also include the kinase domain, the SH3 module binds to a linker connecting the SH2 module to the kinase domain, orienting the SH2 and SH3 domains with respect to each other and the kinase domain, and establishing a structural framework for the regulation of kinase activity in response to protein phosphorylation.

Electron microscopy suggests that LDLR molecules reconstituted into vesicles form extended structures (*38*), and plausible alternative models for global organization of the LDLR have been proposed previously (*39*). Now that recombinant forms of the ligand-binding domain of the LDLR are available (*40, 41*), the potential exists to determine the global organization of individual modules of the LDLR in the intact receptor.

ACKNOWLEDGMENT

We thank Dali Ma for excellent technical assistance in preparing recombinant plasmids, Lynn Kim for preparation of LR5 mutants, and James Wohlschlegel for purification and refolding of unlabeled LR6*. We are also indebted to Susan Pochapsky of the MIT/Harvard Center for Magnetic Resonance and Gregory Heffron of Dr. Gerhard Wagner's laboratory for technical assistance with NMR spectrometers, Dr. Gerhard Wagner for use of NMR spectrometers at Harvard Medical School, and the MIT/Harvard Center for Magnetic Resonance (supported by Grant RR00995 from the NIH) for use of NMR spectrometers housed at MIT. We are grateful to one anonymous reviewer for thoughtful criticisms of the manuscript.

REFERENCES

1. Brown, M. S., and Goldstein, J. L. (1986) *Science 232,* 34−47.
2. Goldstein, J. L., Hobbs, H. H., and Brown, M. S. (1995) in *The Metabolic and Molecular Bases of Inherited Disease* (Scriver, C. S., Beaudet, A. L., Sly, W. S., and D., V., Eds.) Vol. 2, pp 1981−2030, McGraw-Hill Inc., New York.
3. Yamamoto, T., Davis, C. G., Brown, M. S., Schneider, W. J., Casey, M. L., Goldstein, J. L., and Russell, D. W. (1984) *Cell 39,* 27−38.
4. Sakai, J., Hoshino, A., Takahashi, S., Miura, Y., Ishii, H., Suzuki, H., Kawarabayasi, Y., and Yamamoto, T. (1994) *J. Biol. Chem. 269,* 2173-2182.
5. Saito, A., Pietromonaco, S., Loo, A. K., and Farquhar, M. G. (1994) *Proc. Natl. Acad. Sci. U.S.A. 91,* 9725−9729.
6. Kim, D. H., Iijima, H., Goto, K., Sakai, J., Ishii, H., Kim, H. J., Suzuki, H., Kondo, H., Saeki, S., and Yamamoto, T. (1996) *J. Biol. Chem. 271,* 8373−8380.
7. Herz, J., Hamann, U., Rogne, S., Myklebost, O., Gausepohl, H., and Stanley, K. K. (1988) *EMBO J. 7,* 4119−4127.
8. Bates, P., Young, J. A. T., and Varmus, H. E. (1993) *Cell 74,* 1043−1051.
9. Hobart, M. J., Fernie, B., and DiScipio, R. G. (1993) *Biochemistry 32,* 6198−6205.
10. Marazziti, D., Eggersten, G., Fey, G. H., and Stanley, K. K. (1988) *Biochemistry 27,* 6529−6534.
11. Russell, D. W., Brown, M. S., and Goldstein, J. L. (1989) *J. Biol. Chem. 264,* 21682−21688.
12. Daly, N. L., Scanlon, M. J., Djordjevic, J. T., Kroon, P., and Smith, R. (1995) *Proc. Natl. Acad. Sci. U.S.A. 92,* 6334−6338.
13. Daly, N. L., Djordevic, J. T., Kroon, P. A., and Smith, R. (1995) *Biochemistry 34,* 14474−14481.
14. Fass, D., Blacklow, S., Kim, P. S., and Berger, J. (1997) *Nature 388,* 691−693.
15. Goldstein, J. L., and Brown, M. S. (1974) *J. Biol. Chem. 249,* 5153−5162.
16. Atkins, A. R., Brereton, I. M., Kroon, P. A., Lee, H. T., and Smith, R. (1998) *Biochemistry 37,* 1662−1670.
17. Blacklow, S. C., and Kim, P. S. (1996) *Nat. Struct. Biol. 3,* 758−762.
18. Schneider, W. J., Nimpf, J., and Bujo, H. (1997) *Curr. Opin. Lipidol. 8,* 315−319.
19. Bieri, S., Atkins, A. R., Lee, H. T., Winzor, D. J., Smith, R., and Kroon, P. A. (1998) *Biochemistry 37,* 10994−11002.
20. Sambrook, J., Fritsch, E. F., and Maniatis, T. (1989) *Molecular cloning: a laboratory manual*, Cold Spring Harbor Laboratory Press, Plainview, New York.
21. Kunkel, T. A., Roberts, J. D., and Zakour, R. A. (1987) *Methods Enzymol. 154,* 367−382.
22. McIntosh, L. P., and Dahlquist, F. W. (1990) *Q. Rev. Biophys. 23,* 1−38.
23. Studier, F. W., Rosenberg, A. H., Dunn, J. J., and Dubendorff, J. W. (1990) *Methods Enzymol. 185,* 60−89.
24. Peng, Z. Y., and Kim, P. S. (1994) *Biochemistry 33,* 2136−2141.
25. Bers, D. M., Patton, C. W. and Nuccitelli, R. (1994) in *Methods in Cell Biology* (Nuccitelli, R., Ed.) Vol. 40, pp 3−29, Academic Press, San Diego.
26. Piotto, M., Saudek, V., and Sklenar, V. (1992) *J. Biomol. NMR 2,* 661−665.
27. Bodenhausen, G., and Ruben, D. J. (1980) *Chem. Phys. Lett. 69,* 185−189.
28. Bieri, S., Djordjevic, J. T., Daly, N. L., Smith, R., and Kroon, P. A. (1995) *Biochemistry 34,* 13059−13065.

29. Bieri, S., Djordjevic, J. T., Jamshidi, N., Smith, R., and Kroon, P. A. (1995) *FEBS Lett. 371*, 341−344.
30. Djordjevic, J. T., Bieri, S., Smith, R., and Kroon, P. A. (1996) *Eur. J. Biochem. 239*, 214−219.
31. Dirlam-Schatz, K. A., and Attie, A. D. (1998) *J. Lipid Res. 39*, 402−411.
32. Campbell, I. D., and Downing, A. K. (1998) *Nat. Struct. Biol. 5* (Suppl), 496−499.
33. Knott, V., Downing, A. K., Cardy, C. M., and Handford, P. (1996) *J. Mol. Biol. 255*, 22−27.
34. Downing, A. K., Knott, V., Werner, J. M., Cardy, C. M., Campbell, I. D., and Handford, P. A. (1996) *Cell 85*, 597−605.
35. Eck, M. J., Atwell, S. K., Shoelson, S. E., and Harrison, S. C. (1994) *Nature 368*, 764−769.
36. Xu, W., Harrison, S. C., and Eck, M. J. (1997) *Nature 385*, 595−602.
37. Sicheri, F., Moarefi, I., and Kuriyan, J. (1997) *Nature 385*, 602−609.
38. Saxena, K., and Shipley, G. G. (1997) *Biochemistry 36*, 15940−15948.
39. Esser, V., Limbird, L. E., Brown, M. S., Goldstein, J. L., and Russell, D. W. (1988) *J. Biol. Chem. 263*, 13282−13290.
40. Dirlam, K. A., Gretch, D. G., LaCount, D. J., Sturley, S. L., and Attie, A. D. (1996) *Protein Expression Purif. 8*, 489−500.
41. Simmons, T., Newhouse, Y. M., Arnold, K. S., Innerarity, T., and Weisgraber, K. H. (1997) *J. Biol. Chem. 272*, 25531−25536.

BI9821622